J. Fluid Mech. (1985), *vol.* 157, *pp.* 449–470
Printed in Great Britain

A unified bar–bend theory of river meanders

By P. BLONDEAUX AND G. SEMINARA
Istituto di Idraulica, Facoltà di Ingegneria, Università di Genova, Genoa, Italy

(Received 3 April 1984 and in revised form 27 November 1984)

A two-dimensional model of flow and bed topography in sinuous channels with erodible boundaries is developed and applied in order to investigate the mechanism of meander initiation. By reexamining the problem recently tackled by Ikeda, Parker & Sawai (1981), a previously undiscovered 'resonance' phenomenon is detected which occurs when the values of the relevant parameters fall within a neighbourhood of certain critical values. It is suggested that the above resonance controls the bend growth, and it is shown that it is connected in some sense with bar instability. In fact, by performing a linear stability analysis of flow in straight erodible channels, resonant flow in sinuous channels is shown to occur when curvature 'forces' a 'natural' solution represented by approximately steady perturbations of the alternate bar type. A comparison with experimental observations appears to support the idea that resonance is associated with meander formation.

1. Introduction

Theoretical attempts to give a mechanistic justification of fluvial meandering have proliferated in the last two decades. Most of the theories, which derived from the original works of Hansen (1967) and Callander (1969), actually treated the formation of alternate bars in a straight alluvial channel with non-erodible banks. The works of Adachi (1967), Hayashi (1971), Sukegawa (1971), Engelund & Skovgaard (1973), Parker (1975, 1976), Hayashi & Ozaki (1976, 1980) and Fredsøe (1978) have developed an increasingly deeper understanding of the instability process that leads to the flow winding about bars with the channel axis keeping straight. In particular, Fredsøe's theory, which appears to be the most successful attempt, shows that the ingredients necessary to explain the basic bar-instability mechanism are friction, inertial effects involving the transverse velocity, and sediment transport evaluated by taking into account the effect of transverse bed slope. Furthermore, the theory can predict whether an alluvial stream remains straight, tends to develop alternate bars or tends to braid.

In all the above contributions the ability of a stream to develop alternate bars is taken as implying incipient meandering. Recently Ikeda, Parker & Sawai (1981) following ideas originally put forward by Ikeda, Hino & Kikkawa (1976), tackled the problem of meander formation from an apparently different point of view. By relaxing the restraint of fixed sidewalls, Ikeda *et al.* (1981) investigated the stability of channels with sinuous erodible banks and found conditions for the lateral bend amplitude to grow. The main conclusion of this theory is that 'bar' and 'bend' instabilities operate at similar wavelengths when sinuosity is not too large. This would provide justification for the assumption, implicit in previous works, that alternate bar formation eventually leads to a meandering channel with an initial wavelength close to that of alternate bars.

The above results were based on a two-dimensional model of quasisteady shallow-water flow in a sinuous channel with small curvature, which can be shown (see §4) to be formally valid for meander wavelengths much larger than the channel width. Typical bar perturbations may have wavelengths ranging from four to twelve channel widths. Thus, in order to compare more closely the results of the two theories, it would seem more convenient to employ a model for fully developed flow in sinuous channels with small curvature, relaxing the abovementioned condition on the meander length. Indeed a 'bend' theory based on such a model reveals some previously undiscovered features, which lead to the establishment of a connection with 'bar' theories. In fact, there appear to be critical conditions for the flow in the bend such that a resonance phenomenon occurs. We will show that, under these circumstances, curvature forces a 'natural' solution which represents a quasisteady bar perturbation. Thus it emerges that 'bend' instability does not select the most unstable wavelength of 'bar' instability, but rather that which is nearest to resonance for any given set of flow parameters. We show that the wavelengths selected by this mechanism are about three times as large as those predicted by traditional 'bar'-stability theories, and correspond to approximately steady perturbations.

The above findings raise the delicate question of understanding which of the two mechanisms controls the selection of wavelength in the process of meander formation. In fact, there is vast experimental and field evidence of alternate bar formation in approximately straight channels. However, even in the ideal case of a steady-flow regime, the details of the process that leads from the straight configuration with alternate bar propagation to the quasisteady flow in the meandering channel are not clear. The interesting experimental work by Kinoshita & Miwa (1974) has thrown some light on the particular case when the meandering channel is forced to have a constant wavelength equal to that of the alternate bars expected to form. Under these circumstances the above authors show that there is a critical sinuosity beyond which alternate bars are stabilized. However, this finding still leaves unsolved the problem of understanding the transitional process of 'bend' development and its possible interaction with bar propagation. In this respect some interesting field observations were performed by Lewin (1976) on a gravel-bed river whose development from an artificially straightened configuration to a meandering pattern was followed for a period of about one year. The channel was active only occasionally during high-stage flows. The observations showed that a meandering pattern developed with a wavelength which "...came to exceed twice the spacing of initial bars...These features suggest a loosening of the initial dimensional control of bar spacing..." (Lewin 1976, p. 284). Definite conclusions about the wavelength eventually selected by the transitional process following the initial 'bar' perturbation cannot be drawn because the meandering pattern was still developing when artificial restraightening occurred. However, the trend described by Lewin's field observations does suggest that the bend mechanism acts in the sense predicted by the present theory.

An attempt to account for the effect of channel-bed forms of the alternate-bar type on flow in meander bends was performed by Hasegawa & Yamaoka (1980) in a paper that was pointed out to the present authors by one of the referees. The analysis of Hasegawa & Yamaoka (1980) will be discussed in detail in the following sections. It suffices here to say that it does not seem to predict any resonance nor explain the details of the interactions between bar propagation and bend development.

During revision of the present paper, one further interesting contribution (Kitanidis & Kennedy 1984) has been published where an attempt has been made to extract a common cause of the tendency to meander of both alluvial and incised (rock

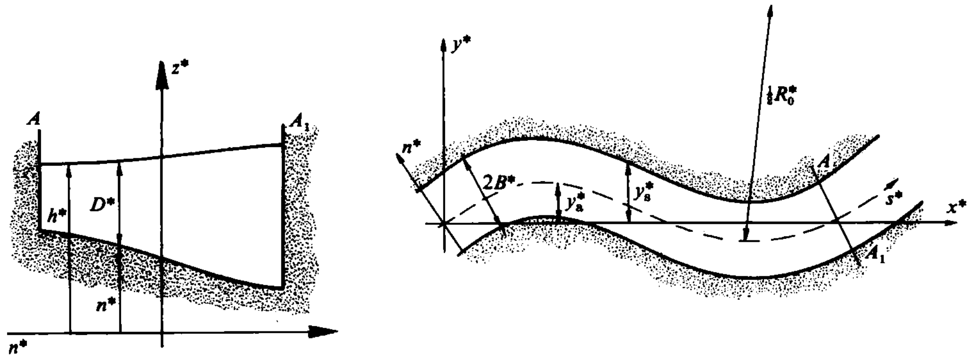

FIGURE 1. Sketch of the channel.

or ice) streams. The analysis of Kitanidis & Kennedy does not allow the channel bottom to vary (i.e. the cross-section is assumed to remain of rectangular form), so that the only factor leading to bend erosion is secondary flow associated with curvature. Though the latter effect is an important common feature of all meandering channels, the present results suggest that in the alluvial case a distinctive feature, bed deformation, plays an equally fundamental role.

The procedure employed in the rest of the paper is as follows. In §2 we formulate the problem of shallow-water flow in sinuous channels with erodible boundaries. In §3 we discuss the relationships employed to describe friction losses, sediment transport and bank erosion. Section 4 is devoted to the formulation and solution of the 'bend' theory. The resonance phenomenon is thus detected, which is interpreted in terms of 'bar' stability theory in §5. Finally (§6) some discussion on the difficulties associated with any attempt to describe the main features of the natural phenomenon concludes the paper.

2. Formulation of the problem

In order to develop a unified approach to 'bar'- and 'bend'-instability theories, we consider the flow in a sinuous channel with constant normal width $2B^*$, small curvature and erodible boundary (figure 1). We note that the 'bar' approach will be recovered in the limit of vanishing curvature and fixed sidewalls.

We assume that the longitudinal channel axis at the level of the undisturbed bed has constant slope S and describes a curve in space, the projection of which onto a horizontal plane is defined by the equation

$$r_0^*(s^*) = R_0^* \, r_0(s^*), \tag{1}$$

where r_0^* is the radius of curvature with characteristic value R_0^* (in the following assumed to be twice the radius at the bend apex) and s^* is a longitudinal coordinate defined along the projected axis. A convenient orthogonal coordinate system is (s^*, n^*, y^*), where n^* is the radial distance from the longitudinal axis and y^* is a vertical coordinate positive in the direction opposite to gravity. We restrict our analysis by the assumption

$$\nu \equiv \frac{B^*}{R_0^*} \ll 1. \tag{2}$$

We point out that in the bend theory, which will be treated in §4, R_0^* and hence ν are slowly varying functions of time. Furthermore, the width of the channel is taken as large enough for the flow to be modelled as two-dimensional, though account will be taken of the influence that the component of secondary flow with zero depth average exerts on sediment transport. In other words, we describe the flow everywhere except for those layers adjacent to the walls where vertical velocities cannot be neglected.

The St Venant equations of quasisteady shallow-water flow in a sinuous channel with slowly varying erodible bottom are written in terms of the above coordinate system in the form

$$V\frac{\partial U}{\partial n}+\frac{r_0(s)}{r_0(s)+\nu n}U\frac{\partial U}{\partial s}+\nu\frac{UV}{r_0(s)+\nu n}=-\frac{r_0(s)}{r_0(s)+\nu n}\frac{\partial H}{\partial s}-\beta\frac{\tau_s}{D},\tag{3a}$$

$$V\frac{\partial V}{\partial n}+\frac{r_0(s)}{r_0(s)+\nu n}U\frac{\partial V}{\partial s}-\nu\frac{U^2}{r_0(s)+\nu n}=-\frac{\partial H}{\partial n}-\beta\frac{\tau_n}{D},\tag{3b}$$

$$\frac{\partial(DV)}{\partial n}+\frac{r_0(s)}{r_0(s)+\nu n}\frac{\partial(UD)}{\partial s}+\nu\frac{DV}{r_0(s)+\nu n}=0,\tag{3c}$$

$$\frac{\partial(F_0^2H-D)}{\partial t}+Q_0\left[\frac{\partial q_n}{\partial n}+\frac{r_0(s)}{r_0+\nu n}\frac{\partial q_s}{\partial s}+\nu\frac{q_n}{r_0(s)+\nu n}\right]=0.\tag{3d}$$

In (3) ρ is water density, U and V are depth-averaged velocity components in the axial (s) and radial (n) directions; τ_s and τ_n are bottom shear stresses; H is water-surface elevation; D is local depth; q_s and q_n are sediment flow-rate components in the axial and radial directions. The variables have been made non-dimensional in the form

$$\left.\begin{aligned}&(U^*,V^*)=U_0^*(U,V),\quad (h^*,D^*)=D_0^*(F_0^2H,D),\\&(s^*,n^*)=B^*(s,n),\quad (\tau_s^*,\tau_n^*)=\rho U_0^{*2}(\tau_s,\tau_n),\\&(q_s^*,q_n^*)=\left[d_s^*\left(\left(\frac{\rho_s}{\rho}-1\right)g\,d_s^*\right)^{\frac{1}{2}}\right](q_s,q_n),\quad t=\frac{U_0^*}{B^*}t^*,\end{aligned}\right\}\tag{4}$$

where U_0^* and D_0^* are average speed and depth for the uniform unperturbed flow, (ρ_s, d_s^*) are sediment density and characteristic size respectively, and F_0 is the unperturbed Froude number. Finally, Q_0 is the ratio between the scale of sediment discharge and the flow rate, and β is a width ratio. We find

$$Q_0=\frac{d_s^*[(\rho_s/\rho-1)\gamma d_s^*]^{\frac{1}{2}}}{(1-p)D_0^*U_0^*},\quad \beta=\frac{B^*}{D_0^*},\tag{5}$$

where p denotes sediment porosity.

The boundary conditions to be associated with the system (3) express the physical requirement that the channel walls be impermeable both to the flow and to the sediment. They read

$$V=q_n=0.\tag{6a, b}$$

We point out that these conditions hold also if the banks are assumed to be erodible, the rate of bank erosion being too small to induce any appreciable effect on the flow field.

Finally, two further integral conditions are required in order to 'close' the problem. They express the requirement that flow rate and average valley slope are not affected by the development of perturbations either of the flow field or of the boundary configuration. These conditions will be made explicit in the following sections, where their validity will be discussed in the context of the perturbation scheme employed to derive the solution.

In order to make any progress with the above problem, we need to formulate expressions that relate shear stresses $\boldsymbol{\tau}$, sediment flow rate $\boldsymbol{q}$ and rate of bank erosion to the flow characteristics. This is discussed in §3.

3. Hydraulic resistance, sediment transport and bank erosion

3.1. *Hydraulic resistance*

We express the shear stress $\boldsymbol{\tau}$ in terms of a friction coefficient C defined by the relationship

$$\boldsymbol{\tau} = (\tau_s, \tau_n) = (U, V)\,(U^2+V^2)^{\frac{1}{2}}\,C. \tag{7}$$

The structure of the dependence of C on the flow parameters is not known for general flow conditions. However, we will take advantage of the fact that the flow to be studied is only slightly perturbed with respect to the case of steady flow in straight channels. Thus we will evaluate C in a neighbourhood of the unperturbed uniform configuration by expanding the function C in Taylor series.

In the *plane-bed* regime we employ Einstein's (1950) formula

$$\frac{1}{C^{\frac{1}{2}}} = 6+2.5\ln\frac{D}{2.5d_{\mathrm{s}}}, \tag{8}$$

where the roughness parameter has been put equal to $2.5d_{\mathrm{s}}^*$ after Engelund & Hansen (1967) and a non-dimensional sediment diameter $d_{\mathrm{s}} = d_{\mathrm{s}}^*/D_0^*$ has been introduced.

For a *dune-covered bed* we follow Engelund & Hansen (1967) and write

$$\Theta' = 0.06+0.4\Theta^2, \tag{9}$$

$$\left(\frac{\Theta}{\Theta' C}\right)^{\frac{1}{2}} = 6+2.5\ln\left(\frac{\Theta'}{2.5\Theta}\frac{D}{d_{\mathrm{s}}}\right), \tag{10}$$

where Θ is Shields parameter defined as

$$\Theta = \frac{\tau_0^*}{(\rho_{\mathrm{s}}-\rho)\,g d_{\mathrm{s}}^*}. \tag{11}$$

Knowledge of the flow behaviour in the *ripple* regime is not sufficient to provide completely reliable resistance laws. However, since some experimental data that will be employed to test the present theory refer to experiments with ripple-covered beds, we decided to employ Richardson, Everett & Simons' (1967) formula, which reads

$$\frac{1}{C_0^{\frac{1}{2}}} = \left(7.66-\frac{0.3}{\Lambda}\right)\log D^* + \frac{0.13}{\Lambda}+11, \tag{12}$$

where

$$\Lambda = \left(\frac{\rho_{\mathrm{s}}-\rho}{\rho}g\Theta d_{\mathrm{s}}^*\right)^{\frac{1}{2}}, \tag{13}$$

and the constants are dimensional and expressed in English units.

3.2. *Sediment transport*

The distinct role of sediment transported as bed load and sediment transported in suspension in connection with bar-instability theory was emphasized by Fredsøe (1978). The above distinction may have an important influence on the stability limits, especially for large values of Θ. However, we will ignore it in the following. Indeed, while complicating the analysis, it is not an essential feature to retain for our main purpose, which is to investigate the relationship between bar and bend instabilities.

In contrast, a crucial effect to be accounted for is the influence that secondary flow and transverse bed slope exert on the direction and intensity of bed-load motion. In this respect a convenient assumption for $\boldsymbol{q}$ is

$$\boldsymbol{q} = (q_s, q_n) = (\cos\delta, \sin\delta)\,\Phi, \tag{14}$$

where Φ is a function describing bed-load transport in the unperturbed uniform configuration and δ is the angle between the average particle path and the s^* direction. This angle differs in general from the angle χ that the local direction of shear stresses forms with the s^* direction.

It can be shown that δ and χ satisfy a relationship of the form

$$\sin\delta = \sin\chi - \frac{r}{\beta}\frac{\partial(F_0^2 H - D)}{\partial n}, \tag{15}$$

which can be obtained by imposing the dynamic equilibrium of a spherical particle uniformly translating along a plane tangent to the bed.

The parameter r was given the form $(\tan\phi)^{-1}$, with ϕ the dynamic friction angle, by Engelund (1974) in his work on bed topography in a meandering channel. The latter expression was found by evaluating the forces acting on a sediment particle and formed the basis for a quite successful prediction of bed topography in a curved alluvial stream. However, as discussed by Parker (1984), some invalid approximations were made to derive the above result. In particular, the bed shear stress was assumed to be parallel to the particle drag.

Kikkawa, Ikeda & Kitagawa (1976) developed a more detailed analysis of the force equilibrium of a bed particle along the longitudinal and transverse directions tangent to the bed. Thus they were able to express $\tan\delta$ and the sum of the local deviation from the longitudinal direction of the fluid velocity at the bed level and of a contribution associated with the transverse bed slope. The latter was of the form $-c\Theta'^{-\frac{1}{2}}\partial(F_0^2 H - D)/\partial n$, with c a function of the lift and drag coefficients of the particle and of various flow parameters.

Engelund (1981) recently reexamined the problem, assuming the particle drag to be parallel to the velocity of the fluid relative to the particle. This led Engelund to express $\tan\Phi$ in terms of Θ' in the form

$$\tan\Phi = 1.6\Theta'^{\frac{1}{2}}. \tag{16}$$

This result was found to be in satisfactory agreement with experimental data. Thus, using the results of Kikkawa *et al.* (1976) and Engelund (1981), recently reconsidered by Parker (1984), we conclude that the parameter r in (15) can be given the form

$$r = r'\Theta'^{-\frac{1}{2}}, \tag{17}$$

with r' a constant in the range 0.5–0.6.

For $\sin\chi$, we write

$$\sin\chi = \frac{V}{(U^2+V^2)^{\frac{1}{2}}} - a\frac{\nu}{\beta}\frac{D}{r_0+\nu n}, \tag{18}$$

distinguishing between a contribution associated with the depth-averaged flow field and a contribution due to the zero-average helical flow occurring in curved channels. The latter has been estimated by employing an expression derived for fully developed flow in circular channels. The constant a ranges between 7 and 12, depending on the turbulence-closure model employed (see Rozovskii 1957; Engelund 1974; De Vriend 1977). We shall assume for a the value 7 (Engelund 1974), which leads to satisfactory agreement with experimental data.

The undisturbed sediment load function Φ will be given a different form depending on the bed configuration.

In the *plane-bed* regime we employ the Meyer–Peter–Müller formula in the form given by Chien (1954), namely

$$\Phi = 8(\Theta - 0.047)^{\frac{3}{2}}. \tag{19}$$

In the ripple and *dune regimes* Engelund & Hansen's (1967) formula will be used:

$$\Phi = \frac{0.05}{C}\,\Theta^{\frac{5}{2}} \tag{20}$$

3.3. *Bank erosion*

Denoting by (x_s^*, y_s^*) the Cartesian coordinates of the bank, the rate of bank erosion (deposit) is defined in the form of Ikeda *et al.* (1981), namely

$$\zeta^* = n_y \frac{\partial y_s^*}{\partial t^*}, \tag{21}$$

where n_y is the cosine of the angle between the normal to the bank and the coordinate axis y^*, and ζ^* is positive (negative) if bank erosion (deposit) occurs. The problem is then that of evaluating ζ^*.

Fortunately, in order to determine the conditions for maximum bend amplification, we do not actually need to quantify ζ^*, but rather to express its dependence on the erosion intensity associated with the flow. The latter is due to the action of shear stresses on the channel banks. Thus we would need a three-dimensional model of the flow field capable of predicting the distribution of shear stresses. However, continuity implies that the vertical component of the flow field close to the banks is driven by the perturbation of the longitudinal component, and is relatively small with respect to the latter. Thus it appears that the major contribution to erosion is associated with the longitudinal shear stress τ_s^*, which is satisfactorily estimated by the present two-dimensional model.

In the following we assume that, for small perturbations of the channel axis, the rate of bank erosion ζ^* is a function of the longitudinal shear stress τ_s^* near the bank.

Thus, following a procedure similar to that developed by Ikeda *et al.* (1981) (p. 368), and defining an 'erosion coefficient' E, we can write

$$\zeta^* = E[\delta\tau_s^*]_{n-1}, \tag{22}$$

where $\delta\tau_s^*$ is the perturbation of τ_s^* due to secondary flow. We implicitly assume that the unperturbed channel configuration is in equilibrium, i.e. erosion is only caused by secondary flow associated with curvature.

It may be useful to point out at this stage that the definition (22) does implicitly account for the expected deepening of the cross-section close to the outer bank. Indeed, an increase of water depth is associated with an increase of longitudinal velocity, which leads to increasing longitudinal bed shear stresses (see (7)). This effect could not be included by Kitanidis & Kennedy (1984), who did not account for bed deformations.

4. Bend theory

We examine a channel whose axis defined as in §2 (see (1)) is assumed to exhibit small-amplitude initial perturbations with respect to the straight configuration.

We want to investigate the conditions required for the above perturbations to grow in time. We Fourier-analyse the function $r_0^{*-1}(s)$ and consider the general Fourier mode defined by

$$r_0^{*-1} = R_0^{*-1}(t)\, e^{i(\lambda_m s - \omega t)} + \text{c.c.}, \tag{23}$$

where λ_m is a non-dimensional meander wavenumber scaled by the half-width B^* of the channel.

Flow in model bends of this kind was studied theoretically and experimentally by Engelund (1974), Hooke (1974) and Gottlieb (1976). More recently Ikeda *et al.* (1981) in their 'bend' theory used an approach similar to that of Engelund. Their analysis will be discussed below in the light of the present formulation.

The solution of the problem posed in §§2 and 3 can be derived, assuming the flow to be developed in the s-direction and taking advantage of the small-ν assumption. A regular expansion in powers of ν could then be set up in the form recently proposed by the present authors (Blondeaux & Seminara 1983*a*). However, this procedure would lead to comparing the bend amplification of meanders characterized by the same curvature ratio and different wavelengths and amplitudes.

It appears to be physically more sensible to compare the amplification rates of meanders with given (small) amplitudes as their wavelengths and curvatures vary.

Thus we assume that the equation of the channel axis can be written in the non-dimensional form

$$y_a = \epsilon(t) \exp i(kx - \omega t) + \text{c.c.}, \tag{24}$$

where y_a, ϵ, k and x are quantities normalized by the half-width B^*, and

$$\epsilon \ll 1. \tag{25}$$

Comparison of (24) and (25) with (23) implies

$$\nu = k^2 \epsilon, \tag{26}$$

$$\lambda_m = k + O(\epsilon^2 k^2), \tag{27}$$

$$s = x + O(\epsilon^2 k^2). \tag{28}$$

Thus it appears that the channel slope S, the average depth D_0^*, the average speed U_0^* and thus the average Froude number F_0 undergo variations due to the bend growth which are $O(\epsilon^2 k^2)$. They are negligible within the present approximation scheme. Moreover, the relationship (26) implies that in order for the amplitude ϵ to be small, ν and k should satisfy the inequality

$$\lambda_m \sim k \gg \nu^{\frac{1}{2}}, \tag{29}$$

i.e. $\epsilon^2 k^2 \ll \nu$.

In other words, a small wavenumber k is described by the present model provided the curvature ratio ν keeps much smaller than k^2.

Having stated the above limits and assuming the flow to be fully developed in the s-direction, we set up the following regular expansion for (U, V, H, D) in powers of ϵ:

$$(U, V, H, D) = (1, 0, H_0, 1) + \epsilon[(\mathscr{F}_1, \mathscr{G}_1, \mathscr{H}_1, \mathscr{D}_1) \exp i(\lambda_m s - \omega t) + \text{c.c.}] + O(\epsilon^2), \tag{30}$$

having assumed the conditions (25)–(29) to be satisfied. If we substitute from (30) and (26) into the governing differential system, at leading order (ϵ^0) we find the uniform-flow solution

$$\frac{\mathrm{d}H_0}{\mathrm{d}s} = -\beta C_0, \tag{31}$$

where β and C_0 are constant within the present approximation scheme. Proceeding to the $O(\epsilon)$ problem, we find

$$\mathrm{L}\begin{bmatrix} \mathscr{F}_1 \\ \mathscr{G}_1 \\ \mathscr{H}_1 \\ \mathscr{D}_1 \end{bmatrix} = \begin{bmatrix} (\mathrm{i}\lambda_{\mathrm{m}} + \chi_0 s_1)\mathscr{F}_1 + (\mathrm{i}\lambda_{\mathrm{m}})\mathscr{H}_1 + \chi_0(s_2 - 1)\mathscr{D}_1 \\ (\mathrm{i}\lambda_{\mathrm{m}} + \chi_0)\mathscr{G}_1 + \dfrac{\mathrm{d}\mathscr{H}_1}{\mathrm{d}n} \\ \dfrac{\mathrm{d}\mathscr{G}_1}{\mathrm{d}n} + (\mathrm{i}\lambda_{\mathrm{m}})\mathscr{F}_1 + (\mathrm{i}\lambda_{\mathrm{m}})\mathscr{D}_1 \\ (\mathrm{i}\lambda_{\mathrm{m}} f_1)\mathscr{F}_1 + \left(\mathrm{i}\lambda_{\mathrm{m}} f_2 + \Phi_0 \dfrac{r}{\beta}\dfrac{\mathrm{d}^2}{\mathrm{d}n^2}\right)\mathscr{D}_1 - \dfrac{F_0^2 \Phi_0 r}{\beta}\dfrac{\mathrm{d}^2\mathscr{H}_1}{\mathrm{d}n^2} + \Phi_0 \dfrac{\mathscr{G}_1}{\mathrm{d}n} \end{bmatrix} = \begin{bmatrix} -\chi_0 n \lambda_{\mathrm{m}}^2 \\ \lambda_{\mathrm{m}}^2 \\ 0 \\ 0 \end{bmatrix}, \tag{32a}$$

$$\mathscr{G}_1 = 0 \quad (n = \pm 1), \tag{32b}$$

$$\frac{\mathrm{d}(F_0^2 \mathscr{H}_1 - \mathscr{D}_1)}{\mathrm{d}n} = -\frac{7}{r}\lambda_{\mathrm{m}}^2 \quad (n = \pm 1). \tag{32c}$$

We point out that the top term in the column vector on the right-hand side of (32a) has not been considered in previous theories. It accounts for the effect of cross-stream variation in leading-order water-surface slope.

It is convenient to write the homogeneous ordinary differential operator L in the form

$$\mathrm{L} = \begin{bmatrix} a_1 & 0 & a_2 & a_3 \\ 0 & a_4 & a_5 \dfrac{\mathrm{d}}{\mathrm{d}n} & 0 \\ a_6 & \dfrac{\mathrm{d}}{\mathrm{d}n} & 0 & a_6 \\ a_9 & a_7 \dfrac{\mathrm{d}}{\mathrm{d}n} & -a_8 F_0^2 \dfrac{\mathrm{d}^2}{\mathrm{d}n^2} & a_{10} + a_8 \dfrac{\mathrm{d}^2}{\mathrm{d}n^2} \end{bmatrix}, \tag{33}$$

the coefficients a_i ($i = 1, 2, \ldots, 10$) being defined by the following relationships:

$$\left.\begin{gathered} a_1 = \mathrm{i}\lambda_{\mathrm{m}} + \chi_0 s_1, \quad a_2 = \mathrm{i}\lambda_{\mathrm{m}}, \\ a_3 = \chi_0(s_2 - 1), \quad a_4 = \mathrm{i}\lambda_{\mathrm{m}} + \chi_0 \\ a_5 = 1, \quad a_6 = \mathrm{i}\lambda_{\mathrm{m}}, \\ a_7 = \Phi_0, \quad a_8 = \Phi_0 \frac{r}{\beta}, \\ a_9 = \mathrm{i}\lambda_{\mathrm{m}} f_1, \quad a_{10} = \mathrm{i}\lambda_{\mathrm{m}} f_2. \end{gathered}\right\} \tag{34}$$

In the above, $\chi_0 = \beta C_0$, and (s_1, s_2) and (f_1, f_2) are the coefficients of the leading-order terms in the expansions for τ_s and Φ in powers of ϵ, namely

$$\tau_s = C_0\{1+\epsilon[(s_1\mathscr{F}_1+s_2\mathscr{D}_1)\exp \mathrm{i}(\lambda_m s-\omega t)+\mathrm{c.c.}]\}+O(\epsilon^2), \tag{35a}$$

$$\Phi = \Phi_0\{1+\epsilon[(f_1\mathscr{F}_1+f_2\mathscr{D}_1)\exp \mathrm{i}(\lambda_m s-\omega t)+\mathrm{c.c.}]\}+O(\epsilon^2), \tag{35b}$$

where

$$\left.\begin{aligned} s_1 &= \frac{2}{1-\Theta_0\mathscr{P}_2}, \quad s_2 = \frac{\mathscr{P}_1}{1-\Theta_0\mathscr{P}_2},\\ f_1 &= \mathscr{P}_4\Theta_0 s_1, \quad f_2 = \mathscr{P}_3+\mathscr{P}_4\Theta_0 s_2,\\ \mathscr{P}_1 &= \frac{1}{C_0}\left(\frac{\partial C}{\partial D}\right), \quad \mathscr{P}_2 = \frac{1}{C_0}\frac{\partial C}{\partial \Theta}, \quad \mathscr{P}_3 = \frac{1}{\Phi_0}\frac{\partial \Phi}{\partial D}, \quad \mathscr{P}_4 = \frac{1}{\Phi_0}\frac{\partial \Phi}{\partial \Theta}.\end{aligned}\right\} \tag{36}$$

The system (32a) is solved below in closed form subject to the boundary conditions (32b, c) and the following integral conditions:

$$\int_{-1}^{1}(F_0^2\mathscr{H}_1-\mathscr{D}_1)\,\mathrm{d}n = 0, \quad \int_{-1}^{1}(\mathscr{F}_1+\mathscr{D}_1)\,\mathrm{d}n = 0. \tag{37a, b}$$

They state that flow rate and average valley slope are not affected by the perturbations either of the flow field or of the bed topography.

Before we proceed to discuss the solution, it seems convenient to make some observations on the approaches employed in previous analyses of the same problem. We first analyse the perturbation scheme employed by Ikeda *et al.* (1981). They solved the equations for the fluid motion by decoupling the n-component of momentum equations from the remaining two equations, stating that the former contributes at first order whereas the latter contribute at second order. However, in the light of the present formulation, it appears that the above procedure is only valid provided λ_m is small (though such that the condition (29) can still be satisfied). In fact, in this case, from (32) one readily finds that $\mathscr{P}_1 = O(\lambda_m)$ and $\mathscr{H}_1 \sim \mathscr{F}_1 \sim \mathscr{D}_1 = O(1)$. However, in order for the perturbation scheme to be rational, we then require that the $O(\epsilon\lambda_m)$ terms retained be much larger than those $O(\epsilon^2)$ neglected, i.e. $\lambda_m \gg \epsilon$. Furthermore, the condition (26) restricts the validity of the analysis to the case of extremely small $o(\lambda_m^3)$ curvatures. Furthermore, in the approach of Ikeda *et al.* the bed profile was assumed rather than found by coupling the sediment motion to the flow field. Also, the quantity $r_0/(r_0+\nu n)$ was not retained in their formulation, and the friction factor was assumed to be constant for small perturbations of the uniform configuration.

The above restrictions can be readily overcome by solving the problem formulated in §§2 and 3 in closed form for an arbitrary λ_m subject to the condition (29), and indeed such an extension is very useful, as anticipated in §1. In fact, a comparison is then justified with bar theories, where the assumption of small λ_m is not made. Furthermore, by coupling the sediment-motion problem to the flow problem no information is lost on the response of the whole system to perturbations. This leads to the detection of the resonance phenomenon mentioned in §1.

The paper by Hasegawa & Yamaoka (1980) treats a problem which reduces to that tackled by Ikeda *et al.* (1981) when the amplitude of the 'pseudobars' considered there vanishes. In this case there are many common features between the above approaches. In fact, both:

do not include continuity equation of sediments and neglect the effect of transverse bed shear stress;

assume the friction factor to be constant in the process of linearization;

neglect the effect of curvature on transverse surface slope (see the right-hand side of the first row of (32*a*)).

However, Hasegawa & Yamaoka take inertia into account in the transverse-momentum equation, and solve the linearized system thus obtained by an approximate procedure, essentially by expanding the solution in Fourier series in the transverse coordinate and truncating the expansion at the leading term. The accuracy of this procedure can be judged by considering that in the forcing terms the quantity n is approximated by $8\pi^{-2}\sin\frac{1}{2}\pi n$ in the interval $[-1,1]$. Indeed, there is no need to resort to any approximation in order to solve the linearized system, even in the complete form considered in the present formulation.

In fact, by simple manipulation the system (32)–(37) is reduced to the following 4th-order non-homogeneous ordinary differential problem for $\mathscr{G}_1$:

$$\frac{\mathrm{d}^4\mathscr{G}_1}{\mathrm{d}n^4}+\Gamma_1\frac{\mathrm{d}^2\mathscr{G}_1}{\mathrm{d}n^2}+\Gamma_2\mathscr{G}_1=\Gamma_0, \tag{38a}$$

$$\mathscr{G}_1=0 \quad (n=\pm 1), \tag{38b}$$

$$\frac{\mathrm{d}^2\mathscr{G}_1}{\mathrm{d}n^2}=\Gamma_3 \quad (n=\pm 1), \tag{38c}$$

where Γ_0, Γ_1, Γ_2 and Γ_3 are the following functions of the coefficients a_i $(i=1,\ldots,11)$:

$$\Gamma_0=\frac{(a_9-a_{10})(a_5a_{11}-a_2\lambda_{\mathrm{m}}^2)a_6}{a_8a_5a_1}, \tag{39a}$$

$$\Gamma_1=\frac{a_{10}-a_9}{a_8}+\frac{(-a_5a_9+F_0^2a_4a_8a_6+a_7a_5a_6)(a_3-a_1)}{a_8a_1a_5}+\frac{a_2a_4a_6}{a_5a_1}, \tag{39b}$$

$$\Gamma_2=\frac{(a_{10}-a_9)a_2a_4a_6}{a_8a_5a_1}, \tag{39c}$$

$$\Gamma_3=\frac{a_6(a_3-a_1)}{a_1}\left(\frac{7}{r}\lambda_{\mathrm{m}}^2+F_0^2\right)-\frac{(a_5a_{11}-a_2\lambda_{\mathrm{m}}^2)a_6}{a_5a_1},\; a_{11}=-\chi_0 n\lambda_{\mathrm{m}}^2 \tag{39d}$$

The system (38*a–c*) is readily solved, and gives

$$\mathscr{G}_1=\frac{\Gamma_0}{\Gamma_2}+\gamma_1\cosh\lambda_1 n+\gamma_2\cosh\lambda_2 n, \tag{40}$$

where
$$\lambda_1=\{\tfrac{1}{2}[-\Gamma_1+(\Gamma_1^2-4\Gamma_2)^{\frac{1}{2}}]\}^{\frac{1}{2}},\quad \lambda_2=\{\tfrac{1}{2}[-\Gamma_1-(\Gamma_1^2-4\Gamma_2)^{\frac{1}{2}}]\}^{\frac{1}{2}}, \tag{41a,b}$$

$$\gamma_1=\frac{\lambda_2^2\Gamma_0/\Gamma_2+\Gamma_3}{(\lambda_1^2-\lambda_2^2)\cosh\lambda_1},\quad \gamma_2=\frac{\lambda_1^2\Gamma_0/\Gamma_2+\Gamma_3}{(\lambda_2^2-\lambda_1^2)\cosh\lambda_2}. \tag{41c,d}$$

It appears that $\mathscr{G}_1$ is an even function of n. Using the solution for $\mathscr{G}_1$, we integrate the second row of (32*a*) and find $\mathscr{H}_1$ in terms of an arbitrary constant. Finally $\mathscr{F}_1$ and $\mathscr{D}_1$ are obtained from rows 3 and 4 of (32*a*). The integral condition (37*a*) then determines the arbitrary constant, which is found to vanish. This leaves $\mathscr{F}_1$ and $\mathscr{D}_1$ as known odd functions of n such that the second integral condition (37*b*) is authomatically satisfied. We find

$$\mathscr{H}_1=\left(\frac{\lambda_{\mathrm{m}}^2}{a_5}-\frac{a_4\Gamma_0}{a_5\Gamma_2}\right)n-\frac{a_4}{a_5}\left[\frac{\gamma_1}{\lambda_1}\sinh\lambda_1 n+\frac{\gamma_2}{\lambda_2\sinh\lambda_2 n}\right], \tag{42a}$$

$$\mathscr{D}_1=\delta_0 n+\delta_1\sinh\lambda_1 n+\delta_2\sinh\lambda_2 n, \tag{42b}$$

$$\mathscr{F}_1=-\delta_0 n-\left(\frac{\lambda_1\gamma_1}{a_6}+\delta_1\right)\sinh\lambda_1 n-\left(\frac{\lambda_2\gamma_2}{a_6}+\delta_2\right)\sinh\lambda_2 n, \tag{42c}$$

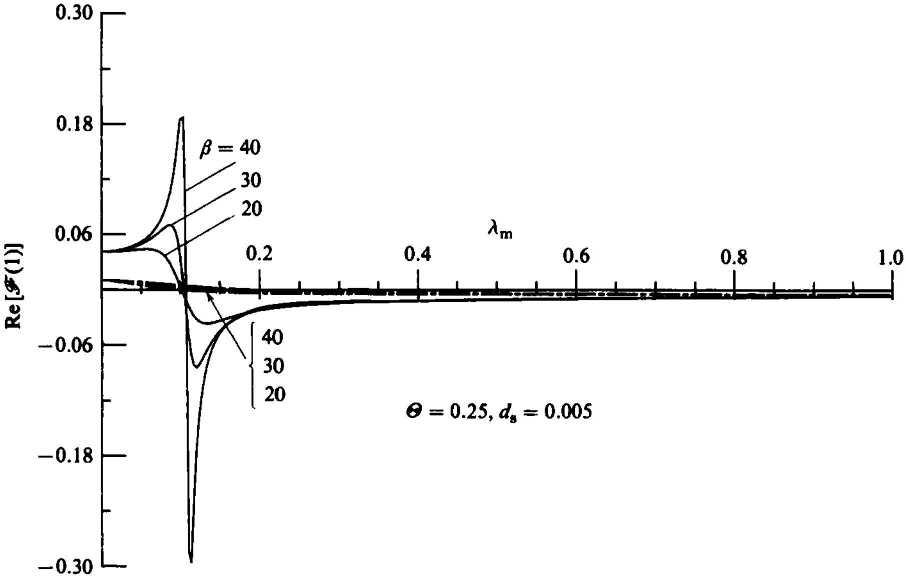

FIGURE 2. Comparison between the present solution (constant ν) (——) and Engelund's (1974) results (–·–·–·–·) for the amplitude of the longitudinal component of perturbation velocity in phase with curvature. Calculations were performed assuming the bed to be plane.

where
$$\delta_0 = \left[-\chi_0 \lambda_m^2 + \frac{a_2}{a_5}\left(\frac{a_4 \Gamma_0}{\Gamma_2} - \lambda_m^2\right)\right]\frac{1}{a_3 - a_1}, \tag{43a}$$

$$\delta_j = \frac{\gamma_j}{a_3 - a_1}\left[\frac{a_2 a_4}{a_5 \lambda_j} + \frac{a_1 \lambda_j}{a_6}\right] \quad (j = 1, 2). \tag{43b}$$

In order to check the validity of the above results, they were compared in a preliminary version of the present paper (Blondeaux & Seminara 1983*b*) with Gottlieb's (1976) experimental findings. The agreement was found to be satisfactory with $r' = 0.5$: a point bar is formed at the convex bank and erosion occurs at the outer bank. Furthermore, bed elevations are predicted fairly accurately, though experimental values are somewhat delayed spatially with respect to the theoretical ones.

In figure 2 we show a comparison with Engelund's (1974) theoretical results performed keeping ν constant (which leads to the monotonic trend of the solution). The quantity that is compared is the real part of $\mathscr{F}_1$, i.e. the amplitude of the longitudinal perturbation velocity in phase with the curvature. It appears that, in a neighbourhood of 'critical' values of wavenumber and width ratio for given Θ and d_s, a resonance phenomenon occurs. Furthermore, as β increases keeping the other parameters constant, resonance shifts to increasingly higher values of λ_m. This feature did not emerge in the approaches of Engelund (1974), Ikeda *et al.* (1981) and Hasegawa & Yamaoka (1980) owing to the approximations already mentioned.

Let us finally come to the crucial question regarding the conditions for maximum amplification of the developing meander. One readily finds

$$\left.\begin{aligned} y_s &= y_a + 1 + O(\epsilon^2 k^2), \\ n_y &\sim 1 + O(\epsilon^2 k^2). \end{aligned}\right\} \tag{44}$$

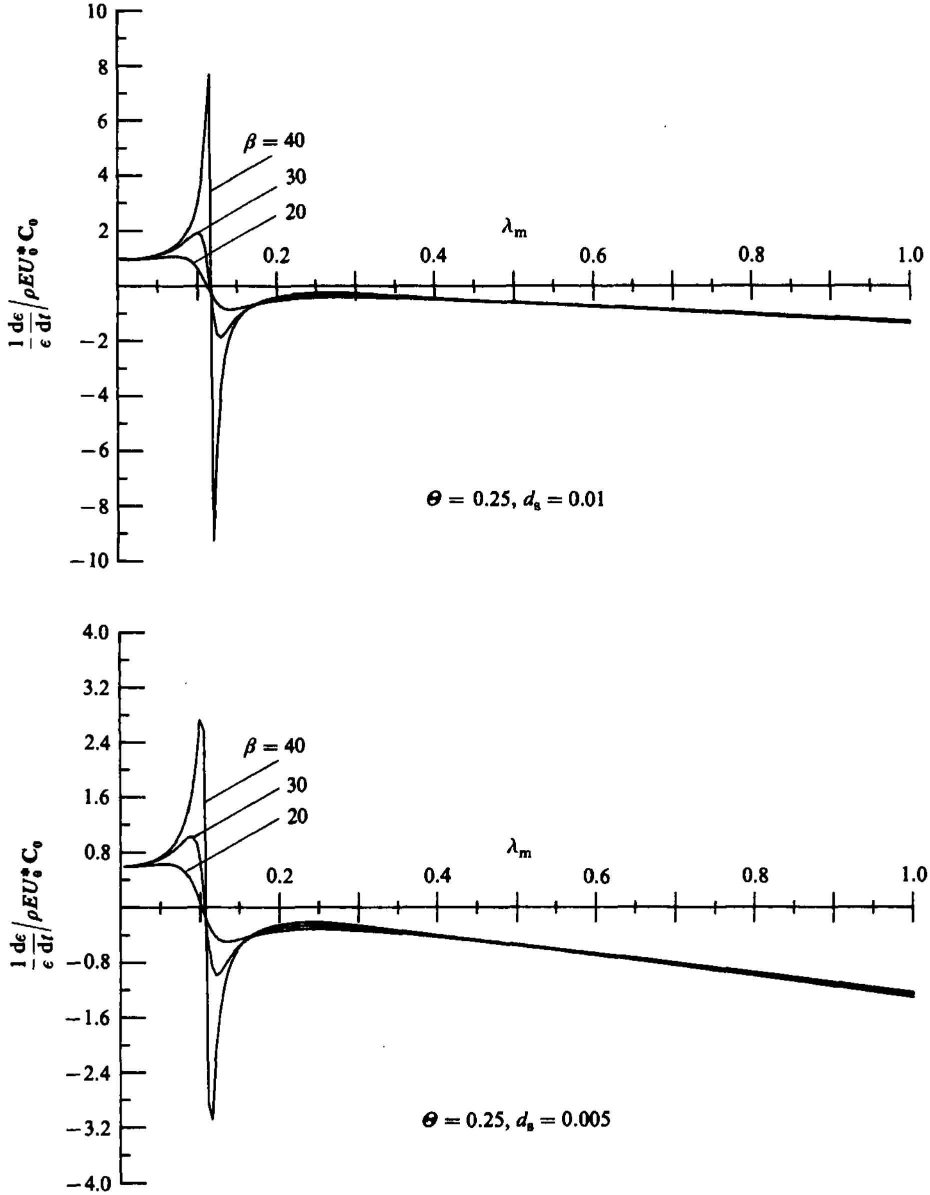

FIGURE 3. The rate of bend amplification is plotted versus λ_m for given values of β, Θ and d_s. Calculations were performed assuming the bed to be plane.

From (21), (22), (24) and (35*a*) it follows that

$$\frac{1}{\epsilon}\frac{d\epsilon}{dt} - i\omega = E\rho U_0^* C_0(s_1 \mathscr{F}_1 + s_2 \mathscr{D}_1)_{n-1}. \tag{45}$$

The rate of bend amplification is then defined by the real part of the right-hand side of (45). Looking for the maximum of the latter quantity as λ_m varies for given Θ, β and d_s leads to selecting the preferred meander wavelength. Figure 3 shows that resonance controls this selection mechanism, and the growth rate increases as friction increases, in agreement with previous theoretical and experimental evidence.

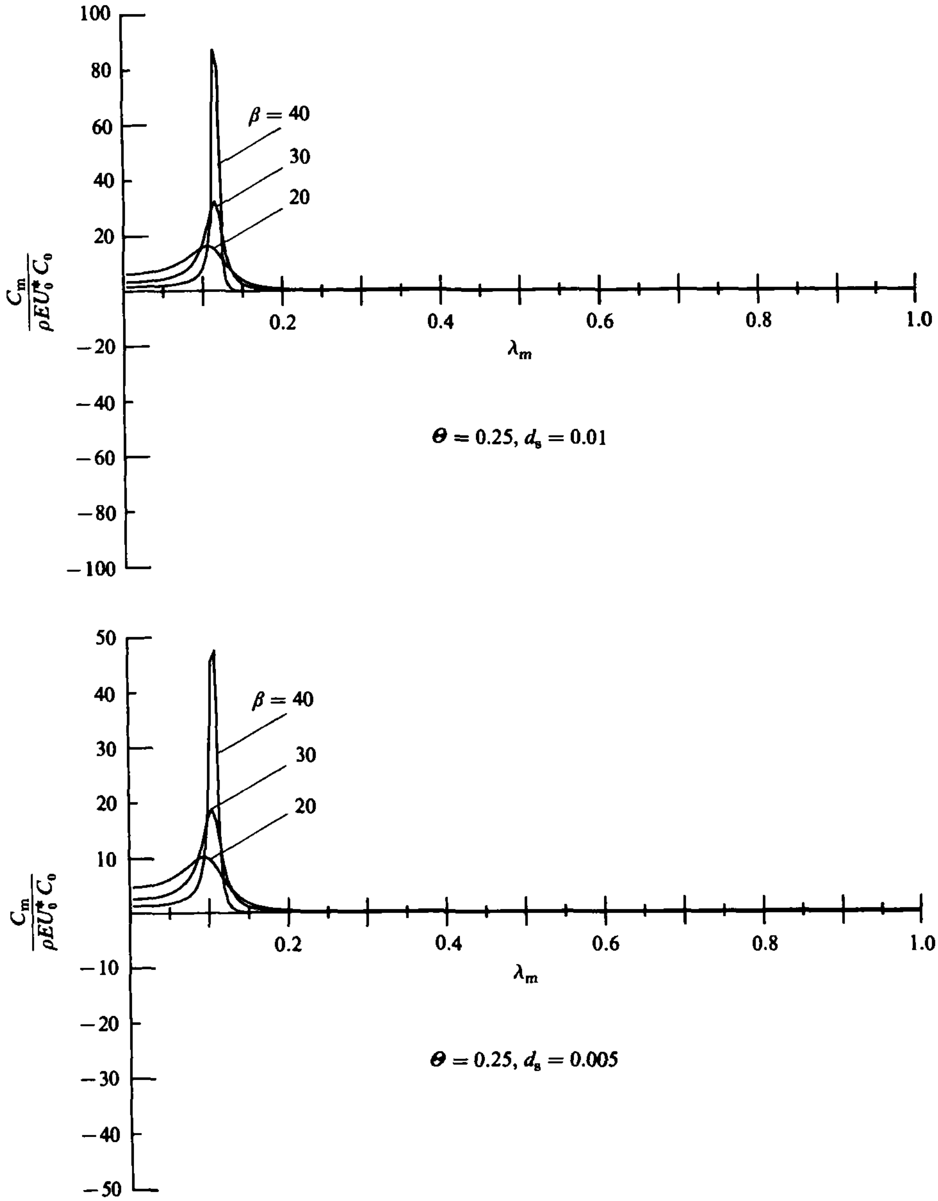

FIGURE 4. The meander-propagation speed (scaled by $E\rho U_0^* C_0$) is plotted versus λ_m for given values of β, Θ and d_s. Calculations were performed assuming the bed to be plane.

The imaginary part of the right-hand side of (45) is equal to $-\lambda_m c_m$, c_m being the non-dimensional meander propagation speed scaled by U_0^*. Figure 4 shows that c_m is positive, as expected, in the range of λ_m close to the resonant peak, thus predicting that meanders migrate downstream.

In figure 5 we plot some results for the present resonant wavelengths predicted by the present theory and compare them with those of Ikeda *et al.* (1981) and Kitanidis & Kennedy (1984). We point out that the discontinuities mark the conditions where higher resonances take over. It also appears that the results of Ikeda *et al.* and Kitanidis & Kennedy smooth out the effect of the resonance as expected. The

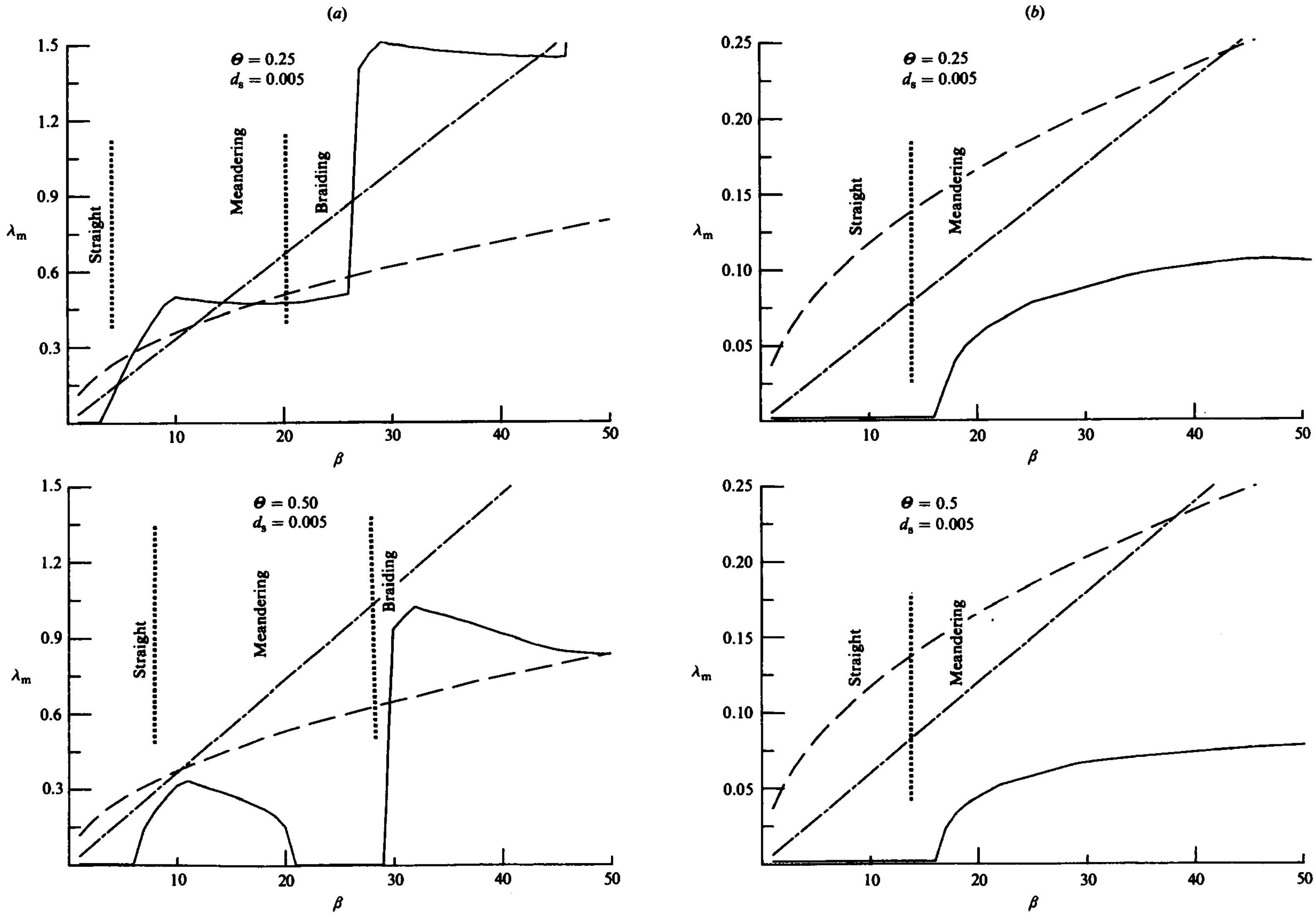

FIGURE 5. The wavenumber corresponding to maximum bend amplification as given by the present theory (——) is plotted versus β, for given values of Θ and d_s, and compared with Ikeda *et al.*'s (1981) (–·–·–) and Kitanidis & Kennedy's (1984) (– – – –) results. Also shown are the ranges of β corresponding to the various morphologic regimes as predicted by the bar theory. (*a*) Calculations performed assuming the presence of dunes. (*b*) Calculations assuming the bed to be plane.

estimate of meander wavelength emerging from figure 5 will be shown to be significantly lower than that arising from bar theories.

It remains to clarify the origin of the above resonance phenomenon. This is discussed in §5.

5. Bar theory: the origin of resonance

In order to answer the question formulated at the end of §4 we need to examine the problem of alternate bar formation in straight alluvial channels. The latter has been the subject of many theoretical investigations, and can be considered as qualitatively solved after Fredsøe's (1978) last remarkable contribution. However, by reconsidering this problem in relation to that tackled in §4, we will show that perturbations of the alternate bar type are forced by curvature in flow in sinuous channels at resonant conditions. These resonant disturbances are not characterized by maximum growth rate nor do they propagate like alternate bars: on the contrary they are steady and non-amplifying.

Let us consider flow in a straight alluvial channel with constant width and non-erodible banks. Under the assumptions described in §§2 and 3, the differential system that governs the problem is readily found by letting ν vanish in the equations discussed there.

We want to investigate the conditions required for the unperturbed uniform flow $(U, V, D, H) = (1, 0, 1, H_0)$ to lose stability to perturbations periodic in the s-direction and small enough for linearization to be a valid approximation. As usual, we perform a normal-mode analysis of the above perturbations and write

$$(U, V, D, H) = (1, 0, 1, H_0) + \epsilon[(u_0, v_0, d_0, h_0)\exp[\mathrm{i}(\lambda_b s - \Omega t)] + \text{c.c.}], \tag{46}$$

where λ_b is a non-dimensional wavenumber of the developing bar and $-\mathrm{i}\Omega$ is a complex number, the real part of which determines the growth rate of the perturbation while its imaginary part defines its non-dimensional frequency. On substituting from (46) into the governing equations, we find the following eigenvalue problem at $O(\epsilon)$:

$$\mathrm{L}_b \begin{bmatrix} u_0 \\ v_0 \\ h_0 \\ d_0 \end{bmatrix} + \begin{bmatrix} 0 \\ 0 \\ 0 \\ \dfrac{-\mathrm{i}\Omega}{Q_0}(h_0 - d_0) \end{bmatrix} = 0, \tag{47a}$$

$$v_0 = \frac{\mathrm{d}(h_0 - d_0)}{\mathrm{d}n} = 0 \quad (n = \pm 1), \tag{47b,c}$$

where L_b is the operator obtained by replacing λ_m with λ_b in the operator L defined by (33). The differential system (47a–c) poses an eigenvalue problem for $-\mathrm{i}\Omega$. We solve it by Fourier-analysing the eigenfunctions (u_0, v_0, h_0, d_0) in the interval $[-1, 1]$ and examining the response of each mode independently. The boundary conditions suggest that

$$(u_0, h_0, d_0) = \begin{cases} (f_0, h_0, d_0)\sin\tfrac{1}{2}\pi mn & (m \text{ odd}), \\ (f_0, h_0, d_0)\cos\pi mn & (m \text{ even}), \end{cases} \tag{48}$$

$$v_0 = \begin{cases} g_0 \cos\tfrac{1}{2}\pi mn & (m \text{ odd}), \\ g_0 \sin\pi mn & (m \text{ even}), \end{cases} \tag{49}$$

m being the parameter that determines the channel pattern. More precisely $m = 1$ corresponds to incipient alternate-bar formation while $m > 1$ implies tendency of the channel to braid. Substituting from (48) and (49) into (47), we end up with an algebraic eigenvalue problem leading to an eigenrelation among the parameters $-\mathrm{i}\Omega$, m, Θ, β and d_s, which reads

$$-\frac{\mathrm{i}\Omega}{Q_0} = -\Phi_0 \frac{r}{\beta} M^2 + \frac{A_1 \lambda_m^3 + \mathrm{i}A_2 \lambda_m^2 + A_3 \lambda_m + \mathrm{i}A_4}{B_0 + \mathrm{i}B_1 \lambda_m + B_2 \lambda_m^2 + iB_3 \lambda_m^3} \lambda_m, \tag{50}$$

where
$$\left.\begin{aligned} A_1 &= f_2 - f_1, \quad A_2 = -A_1 \chi_0, \quad A_3 = (f_2 - \Phi_0) M^2, \\ A_4 &= -A_1 M^2 \chi_0 s_1 - M^2(\Phi_0 - f_1)(s_2 - s_1 - 1)\chi_0, \\ B_3 &= F_0^2 - 1, \quad B_2 = -[\chi_0 + F_0^2 \chi_0 (s_2 - s_1 - 2)], \\ B_1 &= -M^2 + F_0^2 \chi_0^2 (s_2 - s_1 - 1), \quad B_0 = -M^2 \chi_0 s_1, \quad M = \tfrac{1}{2}\pi m. \end{aligned}\right\} \tag{51}$$

The eigenrelation (50) allows one to determine the selected mode m, and its wavelength λ_b, as that characterized by maximum growth rate for given Θ, d_s and β. Incidentally, we notice that the influence of transverse bed slope is clearly exhibited by (50) as the stabilizing effect associated with the first term of its right-hand side. The latter increases as M increases and β decreases. This leads the theory to predict, as Fredsøe (1978) pointed out, the existence of three regimes: straight, i.e. absence of bars ($Re\,(-\mathrm{i}\Omega < 0$ for any m), alternate bars ($m = 1$ is the most unstable mode), braiding (maximum growth rate corresponding to $m > 1$). The above regimes can be associated with distinct regions in the (β, Θ)-plane for fixed d_s. The lines separating different regimes were found to be in good agreement with those given by Fredsøe (1978) for the case $d_s = 10^{-3}$ and no transport in suspension. However, our results appear to depend markedly on the value chosen for d_s. In other words, the attempts to establish criteria to characterize the various morphologic regimes of rivers involving just two parameters (see e.g. Parker 1976; Hayashi & Ozaki 1980; Kishi & Kuroki 1980) does not appear to be adequate.

In order to substantiate our results, we show in figure 6 a comparison between the wavelengths of alternate bars as predicted by the present theory and those experimentally detected by Chang, Simons & Woolhiser (1971), Ikeda (1984) and other Japanese authors whose results are reported in detail by Ikeda (1984). The agreement appears to be satisfactory. Indeed, in some experiments the particle Reynolds number was fairly low, which may influence the particle dynamics. We also point out that the values of Θ were in most cases less than 0.3, whence the role of transport in suspensions was presumably modest as assumed above.

Let us finally come to the crucial point regarding the origin of the resonance phenomenon arisen in our bend theory. A glance at systems (32) and (47) suggests that if $-\mathrm{i}\Omega$ vanishes the system (47) coincides with the homogeneous part of the system (32). Under these conditions, curvature, i.e. the non-homogeneous part of (32), 'forces' a 'natural' solution which represents steady and non-amplifying bar perturbations. Such resonant conditions are not generally met exactly. However, a quasiresonant peak occurs whenever the relevant parameters fall within a neighbourhood of the critical values, as it appears from figure 2. The presence of more than one peak is then readily explained in terms of the different possible bar modes.

The physics behind the resonance phenomenon is very simple. The straight-channel configuration with an unperturbed bed (except for bedforms of lengthscale much smaller than B^*) is not stable in general. This implies that, under suitable and quite common circumstances, a wide spectrum of large-scale bed perturbations may grow

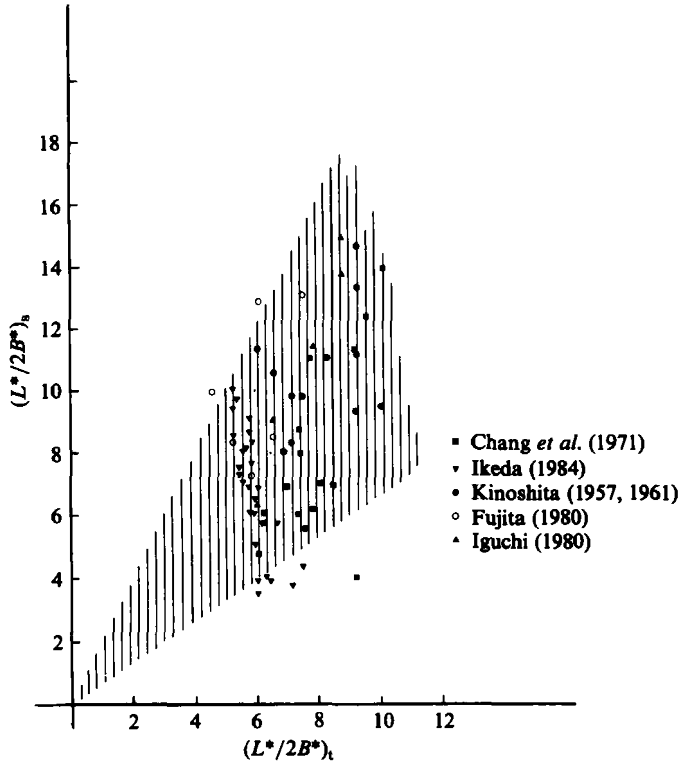

FIGURE 6. The wavelength of alternate bars calculated by the present theory $(L^*/2B^*)_t$ is compared with experimental values $(L^*/2B^*)_s$ obtained by various authors. The dashed region includes data such that the theoretical value differs from the experimental one by an amount which is less than 50% of the latter. Calculations were performed assuming the bed to be plane.

'spontaneously' in time as a result of a classical erosion–deposition process: they correspond to what we called 'natural' solutions. For given flow parameters there generally exists a wavenumber range of 'alternate bar' perturbations, which are characterized by positive growth rates and variable propagation speed (see figure 7). Provided no forcing occurs from any external cause, the wavenumber 'spontaneously' selected (i.e. that actually seen in straight channels) obviously corresponds to those disturbances that exhibit the maximum rate of amplification; they are also found to propagate downstream. However, flow and bed topography in meandering channels also exhibit an 'alternate' character, with scouring and bar deposition occurring alternately close to the outer and inner banks respectively. What distinguishes the 'point-bar' structure of weakly meandering flow from alternate bars is essentially the quasisteady character of the former, i.e. the fact that it neither amplifies nor propagates (except for the slow bend-erosion process). However, it should be noted that among the 'natural modes of vibrations of the system' (the straight channel) there also exist in general quasisteady bar perturbations – those characterized by values of the wavenumbers such that both $\mathrm{Re}(-\mathrm{i}\Omega)$ (the amplification rate) and $\mathrm{Im}(-\mathrm{i}\Omega)$ (the frequency) are 'small' (see figure 7). Then if the wavenumber of the channel falls within the latter range the alternate flow pattern originated by curvature tends to reinforce a 'natural' tendency of the system which leads to resonance.

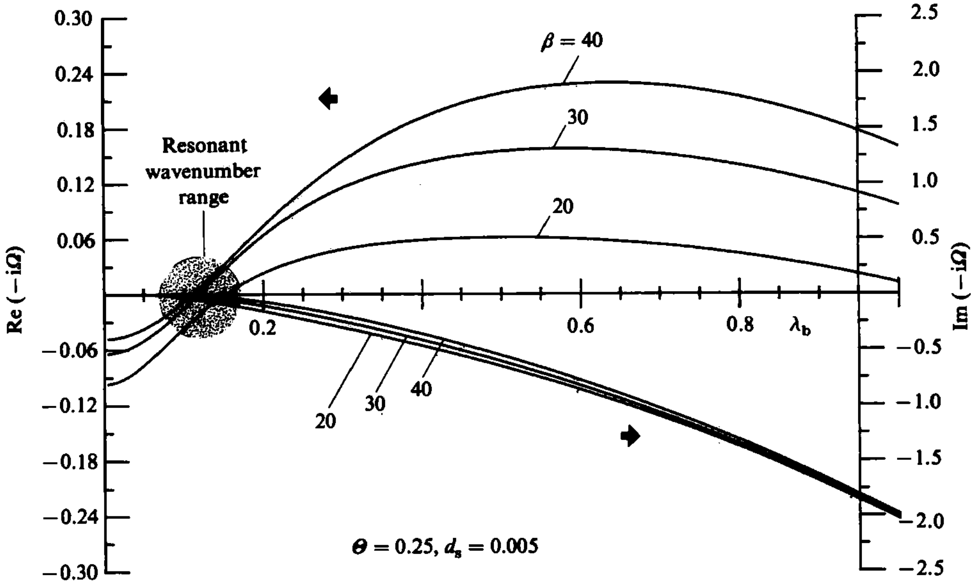

FIGURE 7. The non-dimensional growth rate and propagation frequency of 'bar' perturbations are plotted versus λ_b for given values of β, Θ and d_s. The resonant wavenumber range is also shown.

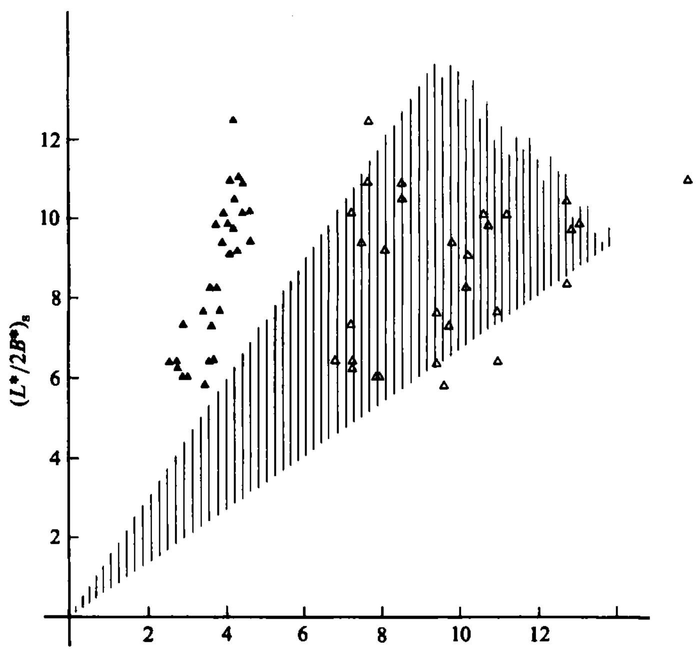

FIGURE 8. The non-dimensional meander wavelengths $(L^*/2B^*)_t$ as predicted by the present 'bend' theory (§4) are compared with the experimental results $(L^*/2B^*)_s$ of Ackers & Charlton (1970) (△). The dashed region includes data such that the theoretical value differs from the experimental one by an amount which does not exceed 30 % of the latter. Also plotted are the wavelengths of alternate bars predicted by the present 'bar' theory (§5) versus experimental values (▲). Calculations were performed assuming the presence of ripples as indicated in the paper by Ackers & Charlton (1970).

The question to be answered is then: in the process of meander formation does the channel select the above wavelength which obviously maximizes bend erosion? In order to get an at least 'indirect' answer to the above question, we finally attempt to compare the wavelength predicted by our bend theory with experimental data and with values predicted for alternate bars. This comparison is shown in figure 8 using data reported by Ackers & Charlton (1970).

Figure 8 appears to support the idea that a 'bend' rather than a 'bar' mechanism prevails. In fact, the observed wavelengths compare uniformly better with the values predicted by our bend theory than with those characteristic of alternate bars. The agreement is to be considered quite satisfactory if account is taken of the uncertainty associated with the evaluation of friction losses, which in most experiments were mainly due to the presence of ripples.

6. Discussion

The analysis developed in the previous sections and the comparison with experimental data seems to support the idea that alternate-bar formation and bend amplification are controlled by two distinct mechanisms: instability in the former case, resonance in the latter.

Furthermore these mechanisms are somewhat interrelated, as discussed previously. Incidentally, it may be of interest to point out that the relation between the latter mechanisms can only be detected if the formulation of the 'bend' theory includes the dependence of both friction factor and bed load function on the flow parameters. In fact, as shown originally by Callander (1969), alternate-bar formation is extremely sensitive to the above dependence. In other words, if C and Φ are assumed to be constant the straight configuration is always found to be stable to 'bar' perturbations and no resonance may occur.

A tentative conclusion that might be drawn from the above findings is that, provided bend amplification is allowed to develop, the transient process starting from the straight configuration initially perturbed by the presence of alternate bars should tend to a steady state determined by the 'bend' mechanism. A laboratory experiment under controlled conditions is ultimately required in order to provide a final check of the above conclusion.

The reader may have noticed that, while laboratory observations have been used to substantiate our theoretical findings, a comparison between theoretical predictions and field data has not been attempted. This is because we feel that such a comparison would suffer from several difficulties associated with various features of the natural phenomenon that are not accommodated in our model.

The main difficulty arises when one is forced to choose a 'representative' discharge of the river to feed in the calculations. By this procedure it is implicitly assumed that the effect of the variable regime of a river can be satisfactorily modelled in terms of a 'formative' discharge. There is not enough experimental or theoretical evidence to justify the above approach, which is then followed on empirical grounds, and this leads to different choices of the formative discharge by various authors, either based on geometrical criteria (bankfull discharge) or on statistical considerations (mean annual discharge). The available data do not always correspond to the same choice, which complicates any attempt at comparison even further.

Moreover, the theory concerns the incipient formation of meanders, whereas field data often refer to fully developed meanders. It has been observed that meander wavelength does not change much as its amplitude grows, but the same statement does not apply to the variations of slope, depth and width ratio. Data found in the literature should often be modified in order to reproduce the initial conditions of the process of meander formation. However, information is not always sufficient to allow such corrections.

Further sources of inaccuracy may be associated with the impact that artificial human actions may have had on the evolution of the river or with constraints imposed on the latter by possible non-uniformities of the geological structure of the valley. These features are often quite difficult to evaluate.

There are also difficulties related to the evaluation of friction losses and sediment transport in actual field conditions and to the important role of suspension load neglected in the present work.

We feel that further research is needed to understand each of the above effects before the ambitious programme of gaining a general understanding of meander formation under natural conditions can be fulfilled.

In this respect substantial improvements of the present model can be accomplished by investigating the effects of relaxing the assumptions of fully developed flow (some steps in this direction have been made by De Vriend & Struiksma 1983), linear interaction between bed topography and flow field, and negligible suspended load. Also, a better description of the flow structure close to the sidewalls and of the way it determines bank erosion is needed.

Finally, we notice that the perturbation scheme employed in our bend theory breaks down close to resonance. It can be shown that an $O(\epsilon^{\frac{1}{3}})$ 'natural' term arises, the amplitude of which can be found by expanding the solution in powers of $\epsilon^{\frac{1}{3}}$ and imposing a solvability condition on the non-homogeneous ('forced') problem found at $O(\epsilon)$.

Grateful thanks are due to Professor G. Parker for constructive criticism and for generously providing us with a translation of the paper by Kinoshita & Miwa (1974) and with a copy of one of his papers as yet unpublished. The authors also wish to thank Professor S. Ikeda for kindly providing some of the data reported in figure 6.

The work has been supported by CNR under grant 83.00155.07 and partially by MPI (National Research Projects).

REFERENCES

Adachi, S. 1967 A theory of stability of streams. In *Proc. 12th Congr. IAHR, Fort Collins, Colorado*, vol. 1, pp. 338–343.

Blondeaux, P. & Seminara, G. 1983*a* Bed topography and instabilities in sinuous channels. In *Proc. ASCE Rivers '83, New Orleans*, pp. 747–758.

Blondeaux, P. & Seminara, G. 1983*b, c* Formazione dei meandri in alvei incoerenti. *Giornata di Studio sugli Alvei con Granulometria Grossolana e Incoerente, Napoli*, parte I e II, pp. 141–180.

Callander, R. A. 1969 Instability and river channels. *J. Fluid Mech.* **36**, 465–480.

Chang, H., Simons, D. B. & Woolhiser, D. A. 1971 Flume experiments on alternate bar formation. *J. Waterways, Harbors, Coastal Engng Div. ASCE* **97**, 155–165.

Chien, N. 1954 In *Proc. ASCE* **80**, 1954.

de Vriend, H. J. 1977 A mathematical model of steady flow in curved shallow channels. *J. Hydraul. Res.* **15**, 37–54.

De Vriend, H. J. & Struiksma, N. 1983 Flow and bed deformation in river bends. In *Proc. ASCE Rivers '83, New Orleans*, pp. 810–828.

Einstein, H. A. 1950 The bedload function for sediment transport in open channel flow. *US Dept Agric. Tech. Bull.* 1026.

Engelund, F. 1974 Flow and bed topography in channel bends. *J. Hydraul. Div. ASCE* **100** (HY11), 1631–1648.

Engelund, F. 1981 The motion of sediment particles on an inclined bed. *Tech. Univ. Denmark ISVA Prog. Rep.* 53, pp. 15–20.

Engelund, F. & Hansen, E. 1967 *A Monograph on Sediment Transport in Alluvial Streams.* Copenhagen: Danish Technical Press.

Engelund, F. & Skovgaard, O. 1973 On the origin of meandering and braiding in alluvial streams. *J. Fluid Mech.* **57**, 289–302.

Fredsøe, J. 1978 Meandering and braiding of rivers. *J. Fluid Mech.* **84**, 609–624.

Gottlieb, L. 1976 Three-dimensional flow pattern and bed topography in meandering channels. *ISVA Tech. Univ. Denmark Series Paper* 11.

Hansen, E. 1967 On the formation of meanders as a stability problem. *Hydraul. Lab. Tech. Univ. Denmark Basic Res. Prog. Rep.* 13, pp. 9–13.

Hasegawa, K. & Yamaoka, I. 1980 The effect of plane and bed forms of channels upon the meander development. *Proc. JSCE* **296**, 143–152.

Hayashi, T. 1971 Study on the cause of meandering of rivers. *Trans. JSCE* **2**, 235.

Hayashi, T. & Ozaki, S. 1976 On dominant wave length in river meanders from the viewpoint of stability theory on beds. In *Proc. 20th Japanese Conf. Hydraul.*, pp. 89–96.

Hayashi, T. & Ozaki, S. 1980 Alluvial bed form analysis – formation of alternating bars and braids. In *Application of Stochastic Processes in Sediment Transport* (ed. T. Kishi & M. Kuroki); *Water Resources Publ., Littleton, Colorado*, pp. 7.1–7.40.

Hooke, R. L. 1974 Shear stress and sediment distribution in a meander bend. *Ungi Rep.* 30, *University of Uppsala, Sweden.*

Ikeda, S. 1984 Prediction of alternate bar wavelength and height. *ASCE J. Hydraul. Engng* **110**, 371–386.

Ikeda, S., Hino, M. & Kikkawa, H. 1976 Theoretical study of the free meandering of rivers. *Proc. JSCE* **255**, 63–73 (in Japanese).

Ikeda, S., Parker, G. & Sawai, K. 1981 Bend theory of river meanders. Part 1. Linear development. *J. Fluid Mech.* **112**, 363–377.

Kikkawa, H., Ikeda, S. & Kitagawa, A. 1976 Flow and bed topography in curved open channels. *J. Hydraul. Div. ASCE* **102** (HY9), 1326–1342.

Kinoshita, R. & Miwa, H. 1974 River channel formation which prevents downstream translation of transverse bars. *Shinsabo* **94**, 12–17 (in Japanese).

Kishi, T. & Kuroki, M. (eds) 1980 *Application of Stochastic Processes in Sediment Transport; Water Resources Publ., Littleton, Colorado.*

Kitanidis, P. K. & Kennedy, J. F. 1984 Secondary current and river-meander formation. *J. Fluid Mech.* **144**, 217–229.

Lewin, J. 1976 Initiation of bed forms and meanders in coarse-grained sediment. *Geol. Soc. Am. Bull.* **87**, 281.

Parker, G. 1975 Meandering of supraglacial melt streams. *Water Resources Res.* **11**, 551–552.

Parker, G. 1976 On the cause and characteristic scales of meandering and braiding in rivers. *J. Fluid Mech.* **76**, 457–480.

Parker, G. 1984 Lateral bed load transport on side slopes. *ASCE J. Hydraul. Engng* **110**, 197–199.

Richardson, E. W., Everett, V. & Simons, D. B. 1967 Resistance to flow in sand channels. In *Proc. 12th Congr. IAHR, Fort Collins, Colorado*, vol. 1, pp. 141–161.

Rozovskii, I. L. 1957 *Flow of Water in Bends of Open Channels.* Kiev: Acad. Sci. Ukhranian SSR.

Sukegawa, N. 1971 Conditions for the occurrence of river meanders. *Trans. JSCE* **2**, 257–261.